Am J Transl Res 2020;12(6):2554-2569
www.ajtr.org /ISSN:1943-8141/AJTR0103790

Original Article

CircAPLP2 regulates the proliferation and metastasis of colorectal cancer by targeting miR-101-3p to activate the Notch signalling pathway

Han-Bing Wu[1*], Shi-Si Huang[3*], Chang-Geng Lu[1*], Shao-Dong Tian[1], Ming Chen[2]

[1]Department of Oncology, The First People's Hospital of Huaihua City, Huaihua 418000, Hunan, P. R. China; [2]Department of Gastroenterology, The First People's Hospital of Huaihua City, Huaihua 418000, Hunan, P. R. China; [3]Department of Oncology, Central South University Xiangya School of Medicine Affiliated Haikou Hospital, Haikou 570208, P. R. China. [*]Equal contributors.

Received October 21, 2019; Accepted April 30, 2020; Epub June 15, 2020; Published June 30, 2020

Abstract: Colorectal cancer (CRC) is one of the most commonly diagnosed cancers, and it has a poor prognosis. Emerging evidence shows that circular RNAs (circRNAs) may act as good therapeutic targets for cancers due to their abundance and stability. However, their regulatory role in CRC needs further investigation. This study revealed that circAPLP2 was upregulated and miR-101-3p was downregulated in CRC tissues and cells compared to normal controls. Knockdown of circAPLP2 and overexpression of miR-101-3p inhibited the cell proliferation, migration and invasion and induced the apoptosis of CRC cells. circAPLP2 acted as a miR-101-3p sponge to upregulate its target gene Notch1, which activated cascades of proliferation- and metastasis-related proteins (c-Myc, cyclin D1, MMP-2 and MMP-9). Additionally, knockdown of circAPLP2 suppressed tumour growth and liver metastases of CRC in nude mice. Taken together, these results indicate that circAPLP2 promotes proliferation and metastasis by targeting miR-101-3p to activate the Notch signalling pathway in CRC, which provides new insights into the mechanisms underlying CRC malignancy and suggests a new therapeutic target.

Keywords: Colorectal cancer, circAPLP2, miR-101-3p, Notch signalling pathway, tumour metastasis

Introduction

As the third most commonly diagnosed cancer, CRC has become a principal cause of death worldwide [1], but incidence and mortality rates are decreasing in developed countries due to new screening methods allowing for early diagnosis and treatment [2]. However, the prognosis of CRC patients remains poor because of the high frequency of metastasis and recurrence and late stage at initial diagnosis [3]. Therefore, discovering new prognostic biomarkers and elucidating the potential molecular mechanisms of CRC may provide improved treatments for patients.

The Notch signalling pathway is imperative to normal cell apoptosis, proliferation, development and differentiation [4]. In humans, the Notch pathway includes five ligands and four receptors [5]. Notch1 is one of the four receptors of the notch pathway [6]. Notch signalling is actively involved in the epithelial to mesenchymal transition (EMT) process, ultimately leading to migration [7] and is also reported to be dysregulated in CRC [4] and to be related to the progression and metastasis of CRC; evidence suggests that Notch1 promotes EMT in CRC [8]. Additionally, high expression of Jagged-1 was reported to be associated with poor prognosis after surgery for CRC [8]. Hes1 increased the invasion of CRC through the STAT3-MMP14 pathway [9]. Thus, these studies suggested a crucial role of the Notch signalling pathway in CRC.

Recently, a novel type of non-coding RNA called circular RNAs (circRNAs) was discovered and has become a research hotspot in the field of RNA [10]. CircRNAs form covalently closed loop structures with neither 5'-3' polarities nor polyadenylated tails [11]. Increasing evidence indicates that circRNAs are highly conserved and stable covalently and closely related to can-

cers; thus, they may act as therapeutic targets and biomarkers due to their abundance and stability [12]. For instance, circ_0075828 promotes bladder cancer cell proliferation throu gh activation of CREB1 [13]. However, circ_0005379 regulates the malignant behaviour of oral squamous cell carcinoma through the EGFR pathway [14]. Additionally, circDDX17 acts as a tumour suppressor in colorectal cancer [15]. circITGA7 inhibits colorectal cancer growth and metastasis by modulating the Ras pathway [16]. However, there are still few studies on the regulatory role of circRNA in CRC at present. Recently, circAPLP2 has been verified to be upregulated in CRC tissues [15]. However, whether circAPLP2 plays a regulatory role in the initiation and progression of CRC is still elusive.

MicroRNAs (miRNAs) are endogenous RNAs approximately 20-22 nt in length involved in regulating multiple physiological biological processes, such as tumorigenesis and metastasis [17]. Increasing evidence suggests that many signalling pathways, including the Notch signalling pathway, could be regulated by miRNAs [18]. Recently, it was reported that miR-101-3p was associated with poorer survival after a diagnosis of colon cancer [19]. miR-101 suppresses CRC cell growth in 3D, hypoxic survival and invasive potential [20]. Additionally, low serum levels of miR-101 are associated with poor prognosis of CRC patients after curative resection, indicating its potential prognostic function [21]. To date, there is no report on the direct targeting of the Notch signalling pathway by miR-101. In our previous bioinformatics analysis, a binding site for miR-101-3p on circAPLP2 and Notch1 was discovered. Therefore, it is speculated that circAPLP2 may promote the Notch1-mediated Notch signalling pathway by targeting the inhibition of miR-101-3p, thereby promoting CRC proliferation and metastasis.

Here, circAPLP2 is identified as an oncogene that is upregulated in CRC and sponges endogenous miR-101-3p to promote Notch1 expression and activate the Notch signalling pathway, thereby regulating CRC proliferation and metastasis. Our findings reveal a novel mechanism underlying the involvement of circAPLP2 in CRC progression and support that circAPLP2 serves as a potential biomarker and therapeutic target for CRC.

Materials and method

Patient tissues

Forty-two paired CRC and adjacent normal tissues were obtained from patients during surgery at The First People's Hospital of Huaihua. All samples were directly snap-frozen in liquid nitrogen or stored at -80°C. This study was approved by the ethics committee of The First People's Hospital of Huaihua.

Cell cultures

Human colorectal cancer cell lines (LoVo, HCT-116, SW620, SW480) and a normal colon epithelial cell line (FHC) were all purchased from American Type Culture Collection (ATCC, USA). Cells were cultured in Dulbecco's modified Eagle's medium (DMEM) supplemented with 10% foetal bovine serum (FBS, Gibco, USA). Cells were cultured in a humidified atmosphere of 5% CO_2 at 37°C.

Cell transfection

miR-101-3p mimics and inhibitors as well as their negative controls were purchased from GenePharma (GenePharma, China). miR-101 mimics or inhibitor (25 nM) were transfected into target cells with the help of Lipofectamine 2000 (Invitrogen, USA). Knockdown of circAPLP2 was achieved by sh-circAPLP2 (2 μg, GenePharma, China). After seeding in 6-well plates, the cells were transfected following the manufacturer's protocol 24 h later. RNA extraction and Western blot experiments were conducted at 48 h after transfection.

Cell apoptosis analysis by flow cytometry assay

The Annexin V-FITC Apoptosis Detection Kit (KeyGen Biotech, China) was used to analyse cell apoptosis following the manufacturer's instructions. Briefly, cells were stained with propidium iodide (PI) and FITC. Then, FACS Canto II (BD Biosciences, USA) was used to perform flow cytometry, and BD FACSDiva Software (BD Biosciences, USA) was used to analyse the data.

Colony formation assay

LoVo and SW620 cells were seeded into 6-well plates and cultured. Two weeks later, the colo-

nies were fixed with methanol for 10 min and stained with 0.1% crystal violet for 15 min at room temperature. Cell colonies were counted and photographed.

Wound healing assay

Cells were grown to 80% confluence in a 6-well plate with DMEM supplemented with 10% FBS and were scratched with a sterile 200 μl pipette tip to create a wound. Then, cells were washed with PBS to remove floating cells and added to a medium without serum for 48 h. The total distance travelled by the cells at different time points was quantified with NIS-Elements AR 3.1 software (Nikon).

Transwell assay

For the invasion experiment, a 24-well Matrigel-coated Millicell system (BD Biosciences, USA) was used to measure the invasive ability of cells. To measure cell migration, 2×10^4 LoVo and SW620 cells in DMEM were seeded into 24-well Transwell chambers (Corning, USA), with 200 μl serum-free DMEM in the upper chambers and DMEM with 10% FBS in to the lower chambers. Forty-eight hours after incubation, we carefully removed the non-invading cells from the surface and fixed the cells on the bottom in 100% methanol. Then, the cells were stained with 0.5% crystal violet solution. The migrated and invaded cells were quantified by photographing under a microscope (Nikon, Japan). Cell numbers were calculated in five random fields for each chamber, and the average value was calculated. Each experiment was conducted in triplicate.

Luciferase reporter assay

The fragments from circAPLP2 and Notch1 containing the predicted miR-101-3p binding site and its mutant sequence were amplified by PCR and then subcloned into the pmirGLO plasmids (Promega, USA). Then, 50 pmol/well miRNA mimics and 800 ng/well luciferase reporter plasmids were co-transfected into LoVo and SW620 cells. Lipofectamine 2000 (Invitrogen, USA) was used for transfection. Then, the relative luciferase activities were measured via a dual-luciferase assay system (Promega, USA) after transfection for 48 h.

Animal experiments

The xenograft tumour model was established as described before [22]. Briefly, we purchased 5-week-old male BALB/c nude mice from SJA Laboratory Animal Co., Ltd. (Hunan, China). LoVo and SW620 (5×10^6/0.2 mL PBS) cells with or without circAPLP2 knockdown were subcutaneously inoculated into the right flank of each nude mouse. Then, every 5 days, we measured tumour volumes with digital callipers and calculated with the following formula: tumour volume = 1/2 (length × width^2). Thirty days later, we killed the mice, measured the volume and weight of the tumours and harvested the tumour tissues.

To analyse metastasis [23], 2×10^6 cells were inoculated into the tail vein of each mouse. Six weeks later, we killed the mice and excised the livers. We fixed the livers with 4% paraformaldehyde for 0.5 h. Then, we made consecutive tissue sections (4 μm) and stained them with haematoxylin and eosin (H&E). We evaluated micrometastases in livers under a dissecting microscope (Olympus Imaging America Inc., USA). The animal experiments were approved by the Animal Care Committee of The First People's Hospital of Huaihua.

IHC (immunohistochemistry) assay

IHC assays were conducted as described previously [24]. Briefly, we collected tissues, fixed them in neutral formalin, dehydrated them, and embedded them in paraffin. Then, we sliced them into serial sections (5 μm thick), dehydrated them and treated them at room temperature (RT) in 3% hydrogen peroxide for 10 min, followed by high-temperature antigen retrieval. Then, we blocked them with normal nonimmune animal serum, and we allowed the sections to stand at RT for 20 min. We added primary antibodies rabbit anti-Notch1 (1:200, Abcam, USA) and anti-Ki-67 (1:200, Abcam, USA) and incubated them at 4°C overnight. Then, we added biotinylated goat anti-rabbit IgG secondary antibody and incubated them at 37°C for 20 min. Diamino benzidine chromogen (DAB) solution was used to develop a colour reaction. We retained the sections in haematoxylin, dehydrated them, permeabilized them, and mounted them. Finally, we observed them under a microscope.

RNA extraction and real-time PCR

Total RNA from tissues and cells was extracted with Tri-regent (Sigma, USA). Then, first-strand cDNA was generated by the ImProm-II Reverse Transcription System (Promega, USA). Gene-specific primers and the SYBR Premix Ex Taq II kit (Takara, China) were then used to carry out qPCR analysis. The following primer sequences were used: circAPLP2 forward 5'-AGACTGGGAAATGGGAACCT-3', reverse 5'-GAGGTCTCAGTCATGCCACA-3'; miR-101-3p forward 5'-GCGCGCATACAGTACTGTGATA-3', reverse 5'-GTCGTATCCAGTGCAGGGTCCGAGGTATTCGCACTGGATACGACTTCAGT-3'; Notch1 forward 5'-GCACGTGTATTGACGACGTTG-3', reverse 5'-GCAGACACAGGAGAAGCTCTC-3'; U6 forward 5'-CTCGCTTCGGCAGCACA-3' and reverse 5'-AACGCTTCACGAATTTGCGT-3'; and GAPDH forward 5'-CCAGGTGGTCTCCTCTGA-3' and reverse 5'-GCTGTAGCCAAATCGTTGT-3'. Relative fold changes were analysed by the $2^{-\Delta\Delta Ct}$ method, where Ct is the cycle threshold.

Western blot analysis

Cold RIPA buffer (ThermoFisher, USA) containing protease inhibitor cocktail (Roche, Switzerland) was used to harvest and isolate cells. Then, 10% SDS-PAGE was used to separate protein samples. Then, protein samples were transferred to polyvinylidene difluoride (PVDF) membranes, which were further probed with specific primary antibodies. Horseradish peroxidase (goat anti-rabbit, Abcam) was used as the secondary antibody and incubated at room temperature for 1 h. Antibodies against HSE1, Jagged1, Notch1, c-Myc, cyclin D1, MMP-2, and MMP-9 (1:1000, Abcam, USA) were used. GAPDH (1:5000; ProteinTech, China) was used to perform quantitative autoradiography by the optical density method. SuperPico chemiluminescent substrate (Pierce, USA) was used to visualize signals. ImageJ software (National Institutes of Health, USA) was used to quantify the band intensity.

Statistical analysis

All statistics were analysed by GraphPad Prism 5 software (GraphPad, USA). The results are presented as the mean ± standard deviation. The statistical significance of the differences between two groups was analysed using paired Student's t-test. For comparison of multiple groups, one-way ANOVA was performed. The *P* value was two-sided, and $P < 0.05$ was considered statistically significant.

Results

circAPLP2 and Notch1 are significantly upregulated and miR-101-3p is downregulated in CRC tissues and cells

First, the expression of circAPLP2, miR-101-3p and Notch1 was investigated in 42 pairs of CRC and adjacent normal tissues by qRT-PCR. The results suggested that in CRC tissues, the expression of circAPLP2 and Notch1 was increased, while that of miR-101-3p was decreased (**Figure 1A-C**). Furthermore, circAPLP2 and Notch1 were upregulated, while miR-101 was downregulated in HCT-116, LoVo, SW620 and SW480 CRC cell lines compared with normal colon epithelial cell line FHC (**Figure 1D-F**), indicating a negative correlation between the expression of circAPLP2 and miR-101 in CRC. Since circAPLP2 has the highest expression level in LoVo and SW620 cells, these two cells were selected for subsequent experiments. Additionally, protein expression of the Notch signalling pathway was also detected in those cell lines; **Figure 1G** and **1H** shows that HSE1, Jagged1 and Notch1 were all upregulated in CRC cells compared with normal cells (**Figure 1G** and **1H**). Taken together, circAPLP2 and Notch1 were upregulated in CRC tissues and cells.

circAPLP2 interacts with miR-101-3p and upregulates Notch1 expression in CRC cells

To explore the relationships among circAPLP2, Notch1 and miR-101, we transfected circAPLP2 shRNA into LoVo and SW620 cells, and as shown in **Figure 2A**, circAPLP2 was successfully knocked down, miR-101-3p was upregulated when circAPLP2 was knocked down, and Notch1 was downregulated when circAPLP2 was knocked down. In addition, miR-101-3p mimics and inhibitors were also transfected into LoVo and SW620 cells. **Figure 2B** shows that Notch1 was downregulated when we overexpressed miR-101-3p and that Notch1 was downregulated when miR-101-3p was inhibited. Furthermore, we also predicted potential binding sites between miR-101-3p and circAPLP2 and between miR-101-3p and Notch1 by Starbase database (http://starbase.sysu.edu.

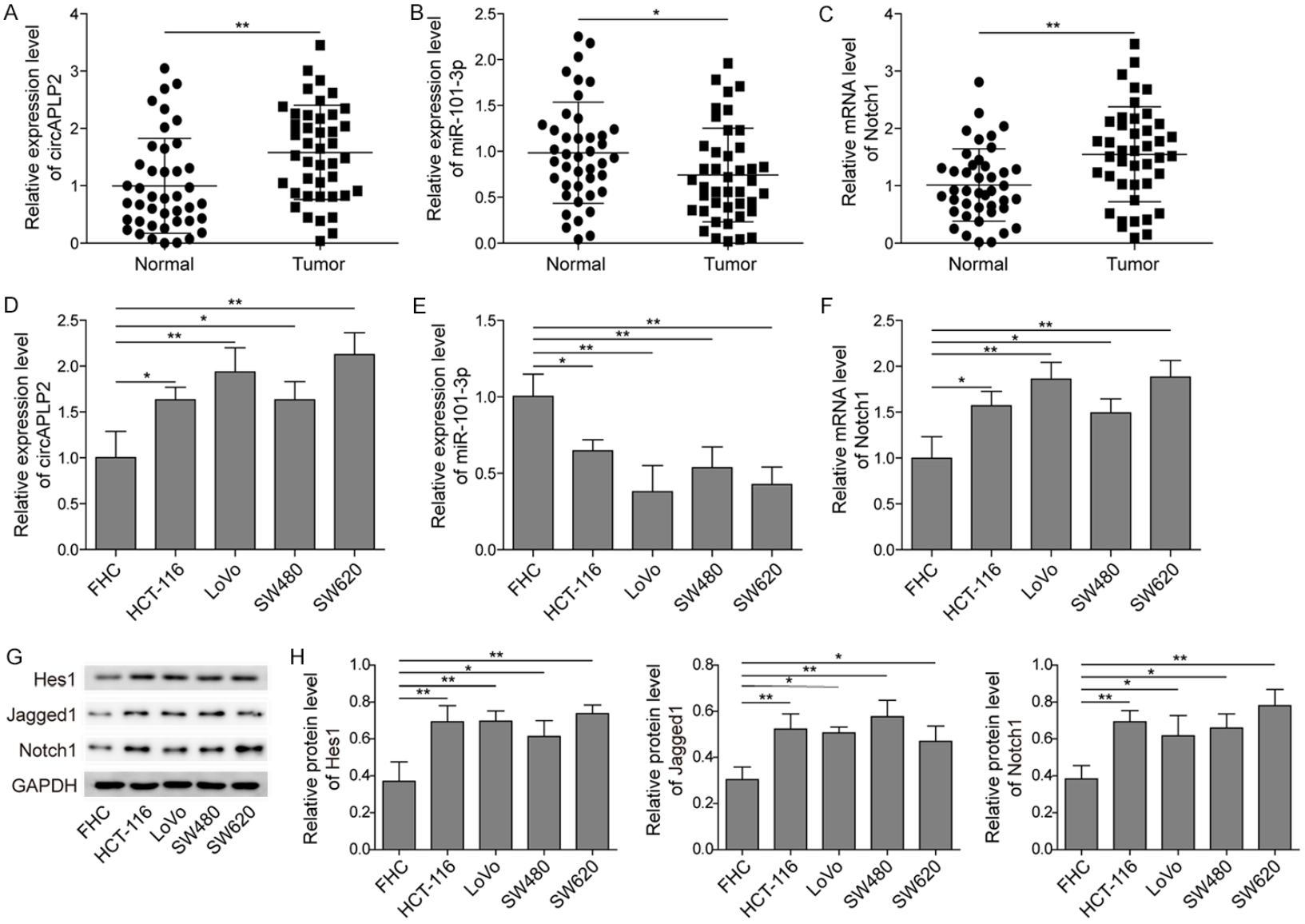

Figure 1. The expression patterns of circAPLP2, miR-101-3p and Notch1 in CRC tissues and cell lines. The expression levels of circAPLP2 (A), miR-101-3p (B) and Notch1 (C) in CRC and adjacent normal tissue samples by qRT-PCR assay. GAPDH or U6 was used for normalization. (N = 42). The expression levels of circAPLP2 (D), miR-101-3p (E) and Notch1 (F) in HCT116, LoVo, SW480, and SW620 CRC cell lines and normal colon epithelial cell line FHC by qRT-PCR assay. GAPDH or U6

was used for normalization. (G) The expression of proteins in the Notch signalling pathway (Hes1, Jagged1 and Notch1) and GAPDH in CRC cells by Western blotting. (H) Greyscale values of Western blot bands are shown in (H); GAPDH was used for normalization. All the results are shown as the mean ± SD (n = 3). *P < 0.05 and **P < 0.01.

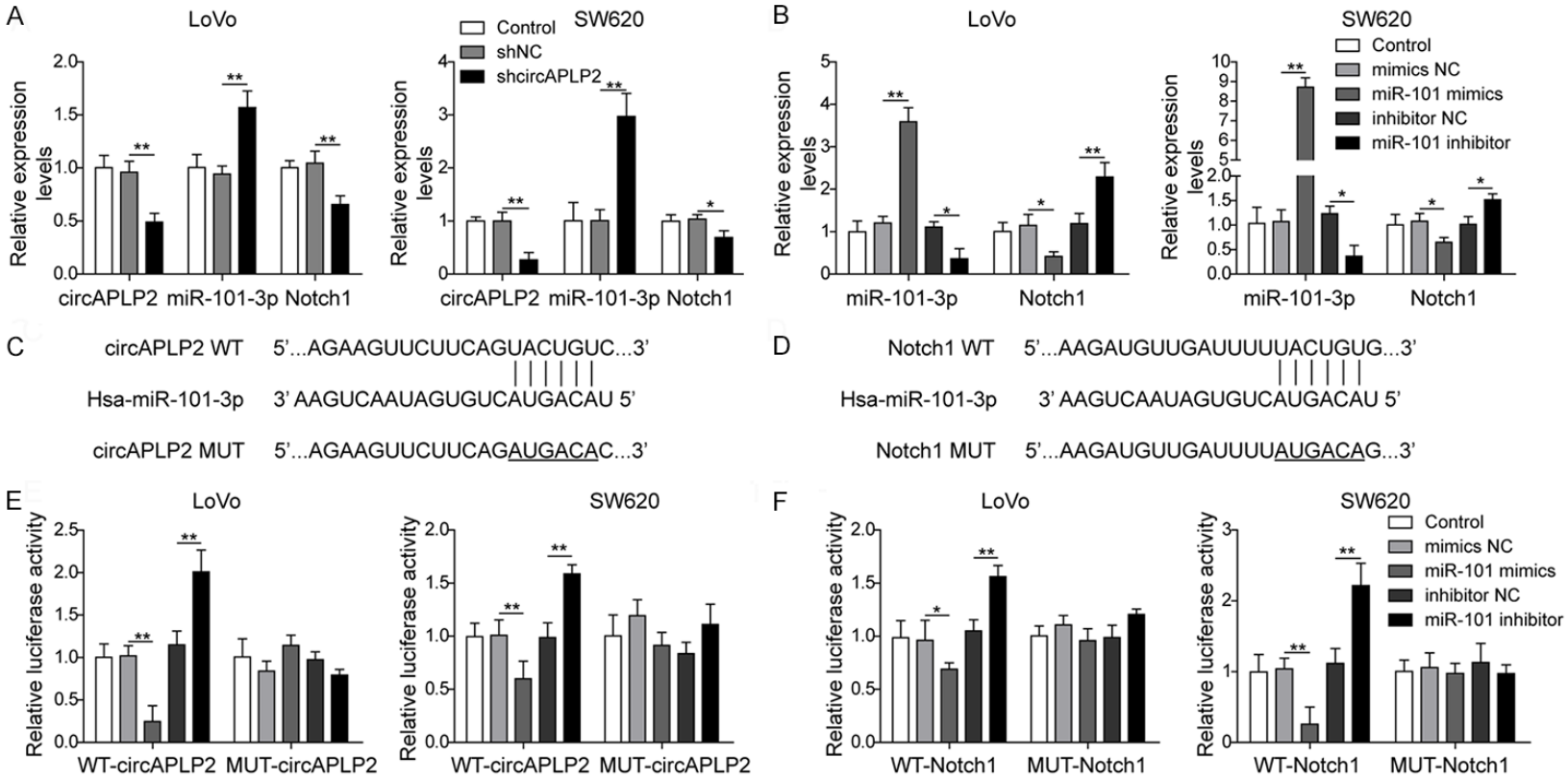

Figure 2. circAPLP2 upregulated Notch1 expression in CRC cells by targeting miR-101-3p. A. The expression levels of circAPLP2, miR-101-3p and Notch1 in LoVo and SW620 cells transfected with sh-NC and sh-circAPLP2 by qRT-PCR. GAPDH or U6 was used for normalization. B. The expression levels of miR-101 and Notch1 in LoVo and SW620 cells transfected with mimics NC, miR-101 mimics, inhibitor-NC and miR-101 inhibitor by qRT-PCR. GAPDH or U6 was used for normalization. C. The binding site of miR-101 on circAPLP2 predicted by Starbase database. D. The miR-101 binding site on Notch1 by predicted Starbase database. E. The luciferase activity of circAPLP2-WT and circAPLP2-MUT in LoVo and SW620 cells transfected with mimics NC, miR-101 mimics, inhibitor-NC and miR-101 inhibitor. F. The luciferase activity of Notch1-WT and Notch1-MUT in LoVo and SW620 cells transfected with mimics NC, miR-101 mimics, inhibitor-NC and miR-101 inhibitor. All the results are shown as the mean ± SD (n = 3). *P < 0.05 and **P < 0.01.

cn/index.php). **Figure 2C** shows the direct binding site between miR-101-3p and circAPLP2, while **Figure 2D** shows the direct binding site between miR-101-3p and Notch1. We also constructed luciferase reporters of circAPLP2 RNA (circAPLP2-WT), Notch1 mRNA (Notch1-WT) and their mutated forms, which did not contain miR-101-3p binding sites (circAPLP2-MUT and Notch1-MUT). Our results demonstrated that miR-101-3p overexpression significantly inhibited the luciferase activity of circAPLP2-WT and Notch1-WT (**Figure 2E** and **2F**) but not the mutated forms (**Figure 2E** and **2F**) in LoVo and SW620 cells. These results fully demonstrated that circAPLP2 promotes Notch1 expression by targeting miR-101-3p.

circAPLP2 knockdown inhibits proliferation and promotes apoptosis of CRC cells through miR-101-3p

We then transfected sh-NC+inhibitor-NC, mimics NC, sh-circAPLP2+inhibitor-NC, miR-101 mimics or sh-circAPLP2+miR-101 inhibitor into LoVo and SW620 cells to investigate the biological role of circAPLP2 in CRC. As shown in **Figure 3A** and **3B**, cell proliferation in the sh-circAPLP2+inhibitor-NC group was significantly decreased compared with that in the sh-NC+inhibitor-NC group, indicating that circAPLP2 knockdown inhibits the proliferation of both cell lines. miR-101-3p overexpression also inhibited cell proliferation compared with that in the mimic NC group (**Figure 3A** and **3B**). When we co-transfected miR-101 inhibitor with sh-circAPLP2, cell proliferation inhibition by circAPLP2 knockdown was successfully rescued (**Figure 3A** and **3B**), indicating that circAPLP2 regulates cell proliferation through miR-101. In the cell apoptosis assay, compared with the negative control cells, both circAPLP2 knockdown and miR-101-3p overexpression cells had significantly increased apoptotic rates in both cell lines (**Figure 3C** and **3D**). Meanwhile, when we co-transfected miR-101 inhibitor with sh-circAPLP2, the elevated apoptosis rate was successfully attenuated (**Figure 3C** and **3D**), indicating that circAPLP2 regulates cell apoptosis through miR-101. Taken together, these results showed that circAPLP2 knockdown inhibits proliferation and promotes apoptosis of CRC cells through miR-101-3p.

circAPLP2 knockdown inhibits the migration and invasion of CRC cells by targeting miR-101-3p

Next, we investigated the regulatory role of circAPLP2 and miR-101-3p in cell metastasis. Wound healing, Transwell migration and invasion assays demonstrated that circAPLP2 knockdown and miR-101-3p overexpression in LoVo and SW620 cells inhibited cell migration and invasion (**Figure 4A-F**). When we co-transfected miR-101 inhibitor with sh-circAPLP2 in both cell lines, this inhibition induced by circAPLP2 knockdown was significantly reversed (**Figure 4A-F**), indicating that circAPLP2 regulated the migration and invasion of CRC cells by sponging miR-101-3p.

circAPLP2 knockdown inhibits the Notch signalling pathway and decreases the expression of metastasis-related proteins by targeting miR-101-3p in CRC cells

The Notch signalling pathway is reported to be related to CRC proliferation and metastasis. To further explore the regulatory role of circAPLP2 on the Notch signalling pathway in CRC cells, we examined the effects of circAPLP2 and miR-101 on the Notch signalling pathway and the levels of proliferation-related proteins. As shown in **Figure 5A** and **5B**, the expression of proteins in the Notch signalling pathway, Hes1, Jagged1 and Notch1, was downregulated by circAPLP2 knockdown and miR-101-3p overexpression in LoVo and SW620 cells. Furthermore, knockdown of miR-101 attenuated the inhibition of the Notch signalling pathway induced by circAPLP2 knockdown (**Figure 5A** and **5B**), demonstrating that knockdown of circAPLP2 inhibited the Notch signalling pathway through regulating miR-101. Moreover, proteins related to cell proliferation and metastasis were also detected. **Figure 5C** and **5D** showed that the expression of proteins c-Myc, cyclin D1, MMP-2 and MMP-9 was downregulated by circAPLP2 knockdown and miR-101 overexpression. The inhibition of the expression of those proteins induced by circAPLP2 knockdown was rescued when we co-transfected miR-101 inhibitor with sh-circAPLP2 in both cell lines (**Figure 5C** and **5D**), indicating that knockdown of circAPLP2 inhibited the signal of cell proliferation and metastasis by sponging miR-101. These results

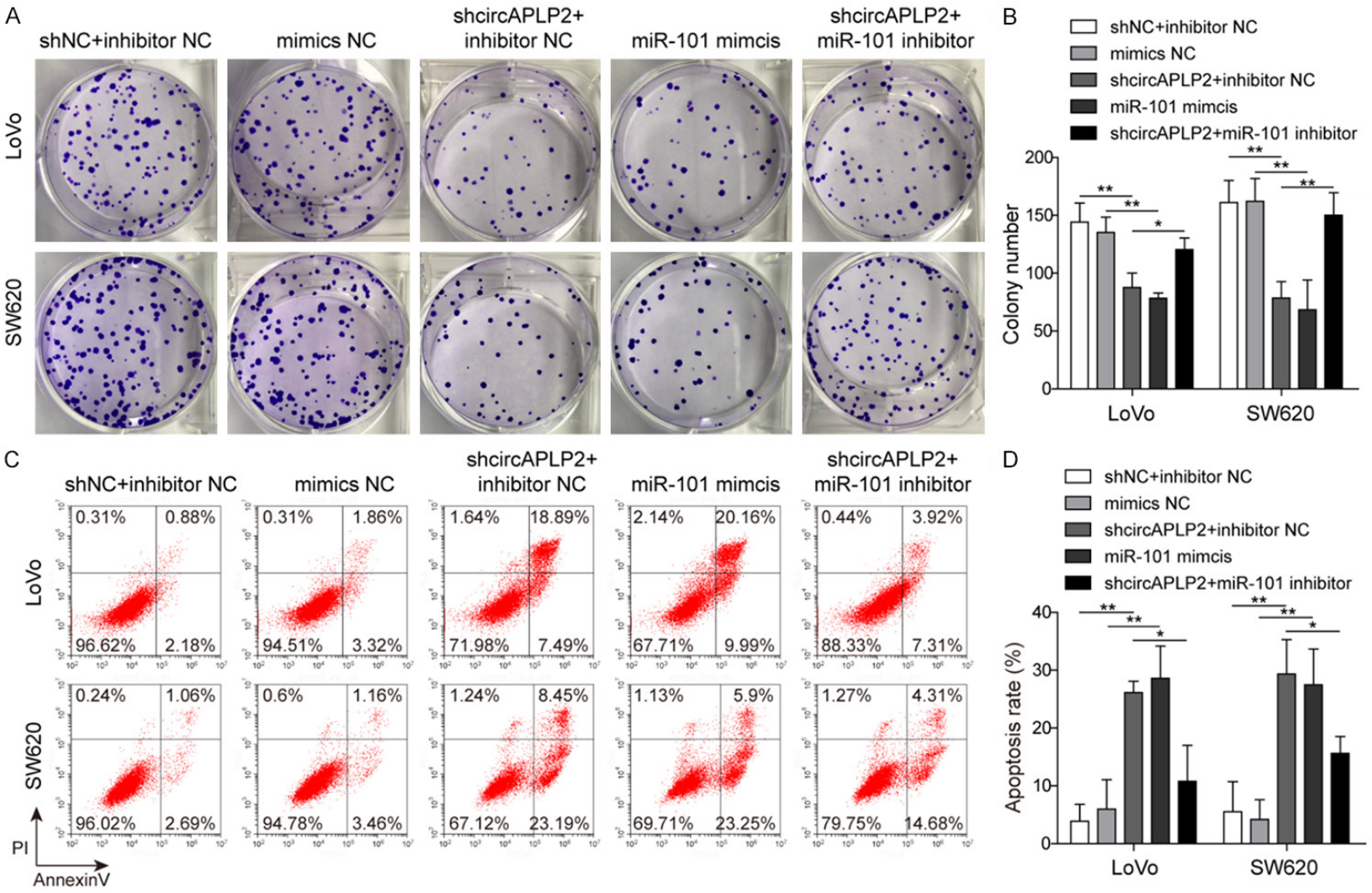

Figure 3. circAPLP2 knockdown inhibited the proliferation and promoted apoptosis of CRC cells through miR-101-3p. (A, B) A colony formation assay was performed to detect the cell proliferation of LoVo and SW620 cells transfected with sh-circAPLP2, miR-101 mimics or miR-101 inhibitor. Representative images of colonies from the indicated cells are shown in (A), and the quantification of colony numbers is shown in (B). (C, D) Flow cytometric analysis of cell apoptosis in LoVo and SW620 cells transfected with sh-circAPLP2, miR-101 mimics or miR-101 inhibitor. Representative flow images are shown in (C), and the quantification of the % of Annexin V^+/PI^+ apoptotic cells is shown in (D). All the results are shown as the mean ± SD (n = 3). *P < 0.05 and **P < 0.01.

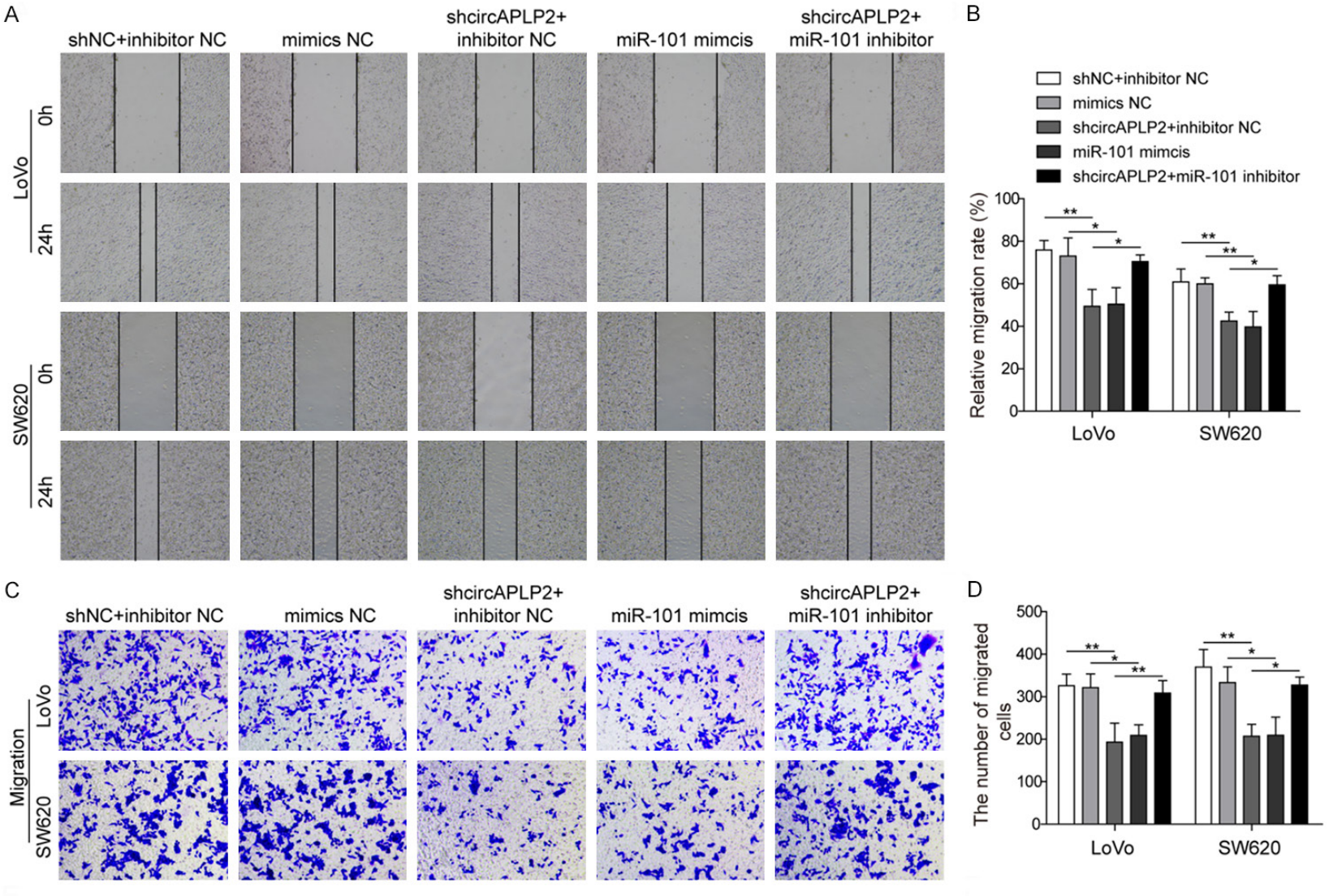
A
shNC+inhibitor NC
mimics NC
shcircAPLP2+ inhibitor NC
miR-101 mimcis
shcircAPLP2+ miR-101 inhibitor
LoVo
0h
24h
SW620
0h
24h
B
shNC+inhibitor NC
mimics NC
shcircAPLP2+inhibitor NC
miR-101 mimcis
shcircAPLP2+miR-101 inhibitor
Relative migration rate (%)
100
80
60
40
20
0
LoVo
SW620
C
shNC+inhibitor NC
mimics NC
shcircAPLP2+ inhibitor NC
miR-101 mimcis
shcircAPLP2+ miR-101 inhibitor
Migration
LoVo
SW620
D
The number of migrated cells
500
400
300
200
100
0
LoVo
SW620

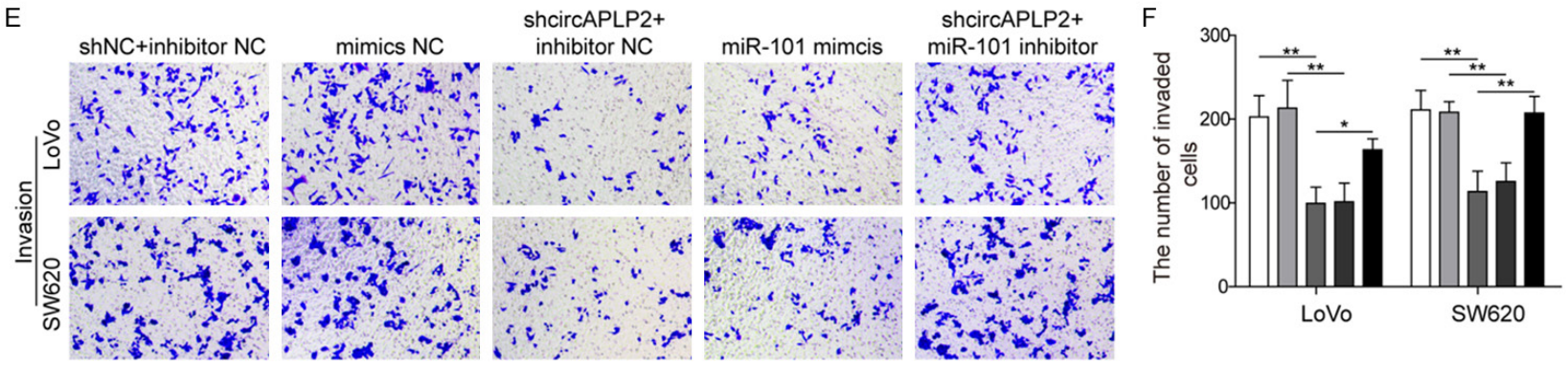

Figure 4. circAPLP2 knockdown inhibited the migration and invasion of CRC cells through miR-101-3p. (A, B) The migration conditions of LoVo and SW620 cells transfected with sh-circAPLP2, miR-101 mimics or miR-101 inhibitor were detected by wound healing assay. Representative images of wound healing from the indicated cells are shown in (A), and the quantification of the migration rate (%) is shown in (B). (C, D) The migration ability of LoVo and SW620 cells transfected with sh-circAPLP2, miR-101 mimics or miR-101 inhibitor was assessed by Transwell assays. Representative images of migrated cells are shown in (C), and the quantification of migrated cells is shown in (D). (E, F) The invasion ability of LoVo and SW620 cells transfected with sh-circAPLP2, miR-101 mimics or miR-101 inhibitor was assessed by Transwell assays. Representative images of invaded cells are shown in (E), and the quantification of invaded cells is shown in (F). All the results are shown as the mean ± SD (n = 3). *P < 0.05 and **P < 0.01.

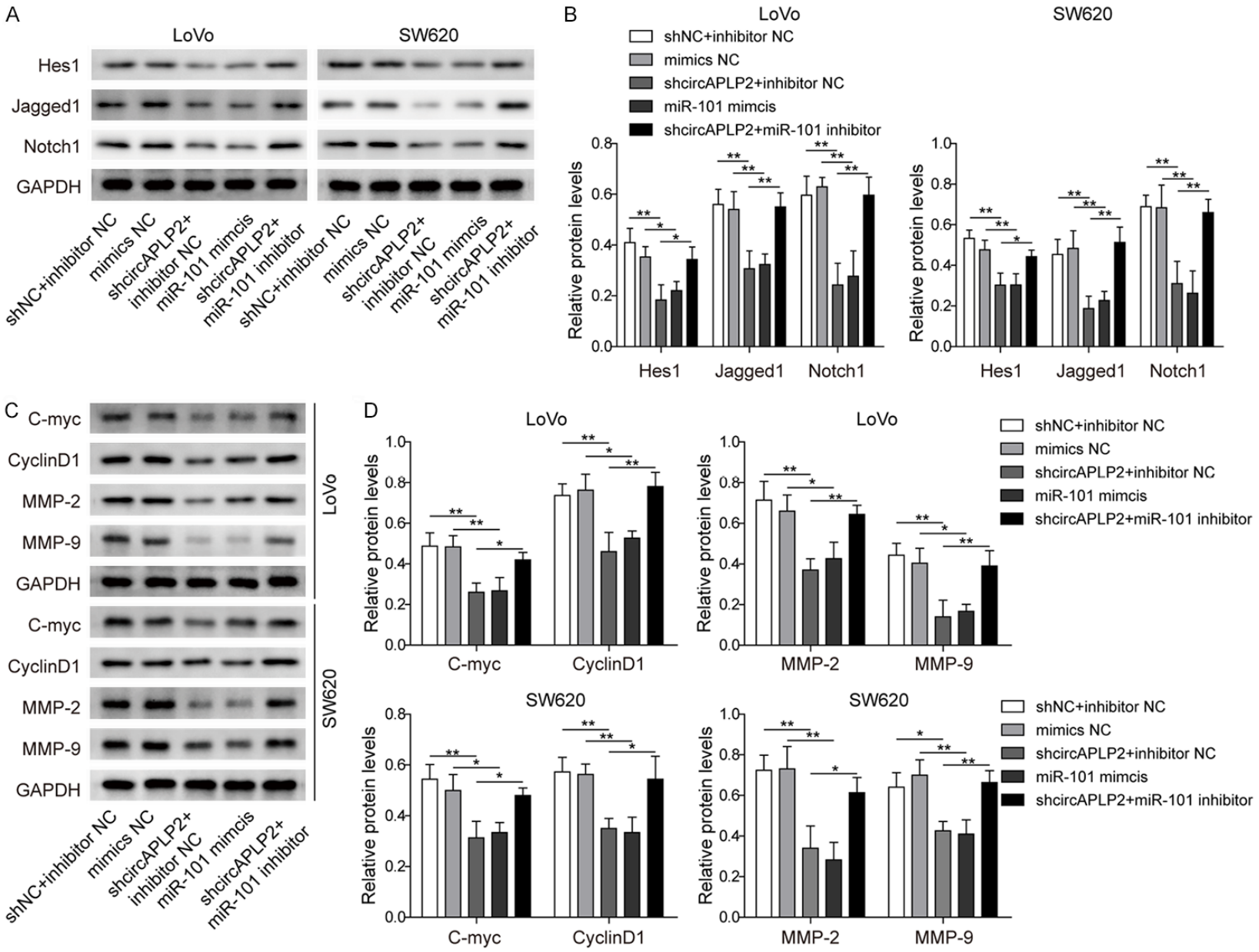
A
LoVo
SW620
Hes1
Jagged1
Notch1
GAPDH
shNC+inhibitor NC
mimics NC
shcircAPLP2+ inhibitor NC
miR-101 mimcis
shcircAPLP2+ miR-101 inhibitor
B
LoVo
SW620
shNC+inhibitor NC
mimics NC
shcircAPLP2+inhibitor NC
miR-101 mimcis
shcircAPLP2+miR-101 inhibitor
Relative protein levels
Hes1
Jagged1
Notch1
C
C-myc
CyclinD1
MMP-2
MMP-9
GAPDH
LoVo
SW620
D
LoVo
SW620
MMP-2
MMP-9

Figure 5. circAPLP2 knockdown repressed the Notch signalling pathway and metastasis-related protein expression through miR-101-3p in CRC cells. (A) The expression of proteins in the Notch signalling pathway (Hes1, Jagged1 and Notch1) was detected by Western blotting in LoVo and SW620 cells transfected with sh-circAPLP2, miR-101 mimics or miR-101 inhibitor. (B) Greyscale values of Western blot bands are shown in (A), and GAPDH was used for normalization. (C) The expression levels of proliferation- and metastasis-related proteins (c-Myc, cyclin D1, MMP-2 and MMP-9) and GAPDH in LoVo and SW620 cells transfected with sh-circAPLP2, miR-101 mimics or miR-101 inhibitor were assessed by Western blotting. (D) Greyscale values of Western blot bands are shown in (C), and GAPDH was used for normalization. All the results are shown as the mean ± SD (n = 3). *P < 0.05 and **P < 0.01.

demonstrated that knockdown of circAPLP2 represses the Notch signalling pathway and decreases the expression of metastasis-related protein by targeting miR-101, thereby inhibiting CRC tumorigenesis and metastasis.

circAPLP2 knockdown suppresses tumour growth and liver metastases of CRC in nude mice

The xenograft mouse models were then established by subcutaneously injecting LoVo cells and SW620 cells transfected with circAPLP2 shRNA or NC shRNA to further assess the regulatory role of circAPLP2 *in vivo*. As shown in **Figure 6A-C**, circAPLP2 knockdown markedly reduced tumour volume and weight compared to that in the control group. The expression levels of circAPLP2 and Notch1 were markedly reduced while miR-101 was significantly increased in xenografts derived from sh-circAPLP2 (**Figure 6D**). Ki-67 staining in xenograft tumours was also detected by IHC and was downregulated in the circAPLP2 knockdown group compared to the control group, indicating the inhibition of tumour proliferation (**Figure 6E**). **Figure 6F**, **6G** shows that circAPLP2 knockdown could decrease the expression levels of Hes1, Jagged1 and Notch1, indicating inhibition of the Notch signalling pathway in tumour tissues. Most importantly, liver tissues were harvested from nude mice, and metastasis was examined. Metastasis to the liver was observed in varying degrees in the nude mice of different groups. The circAPLP2 knockdown group showed fewer liver metastases and a reduction in metastatic nodules in liver tissues (**Figure 6H** and **6I**). Collectively, the nude mouse experiments showed that knockdown of circAPLP2 inhibits tumour formation and liver metastasis by repressing the Notch signalling pathway by targeting miR-101-3p.

Discussion

As a leading cause of cancer-related death worldwide, CRC has a high frequency of recurrence and distant metastasis [25]. Recently, some circRNAs were suggested to play regulatory roles in CRC metastasis. For instance, circRNA_103809 was shown to regulate cell proliferation and migration in CRC via the miR-532-3p/FOXO4 axis [26]. circHIPK3 was reported to promote CRC growth and metastasis by sponging miR-7 [22]. Additionally, circ_000069 was verified to upregulate and promote cell proliferation, migration, and invasion in CRC [27]. Here, elevated expression of circAPLP2 was found in both CRC tissues and cells. Mechanistically, circAPLP2 knockdown inhibited proliferation, migration, and invasion in CRC via the miR-101/Notch axis both *in vitro* and *in vivo*. Though circAPLP2 was verified to be upregulated in CRC compared with normal mucosa tissues, whether it could promote CRC progression was not reported [15]. Thus, our study is the first to demonstrate a regulatory role of circAPLP2 in CRC and to elucidate the exact underlying molecular mechanisms, suggesting a new therapeutic target for combating CRC metastasis.

miR-101-3p is a tumour-suppressive miRNA and is expressed at low levels in several cancer types involved in many biological processes, such as cell apoptosis, proliferation, migration and invasion [28]. A recent study showed that miR-101-3p was associated with poor survival in CRC patients after diagnosis [19], and low serum levels of miR-101-3p were associated with poor prognosis in CRC patients after curative resection [10]. Emerging reports have also suggested that miR-101 acts as an important regulator during the process of EMT. miR-101-3p inhibits EMT and metastasis in glioblastoma by targeting TRIM44 [29]. miR-101-3p also inhibits EMT and invasion-metastasis in serous ovarian cancer by regulating ZEB1 expression [30]. In addition, miR-101-3p inhibits the proliferation and metastasis of bladder cancer cells by targeting EZH2 [31]. However, there is no report in which miR-101-3p is reported to regulate invasion and metastasis by targeting Notch1. In this study, miR-101-3p was shown to

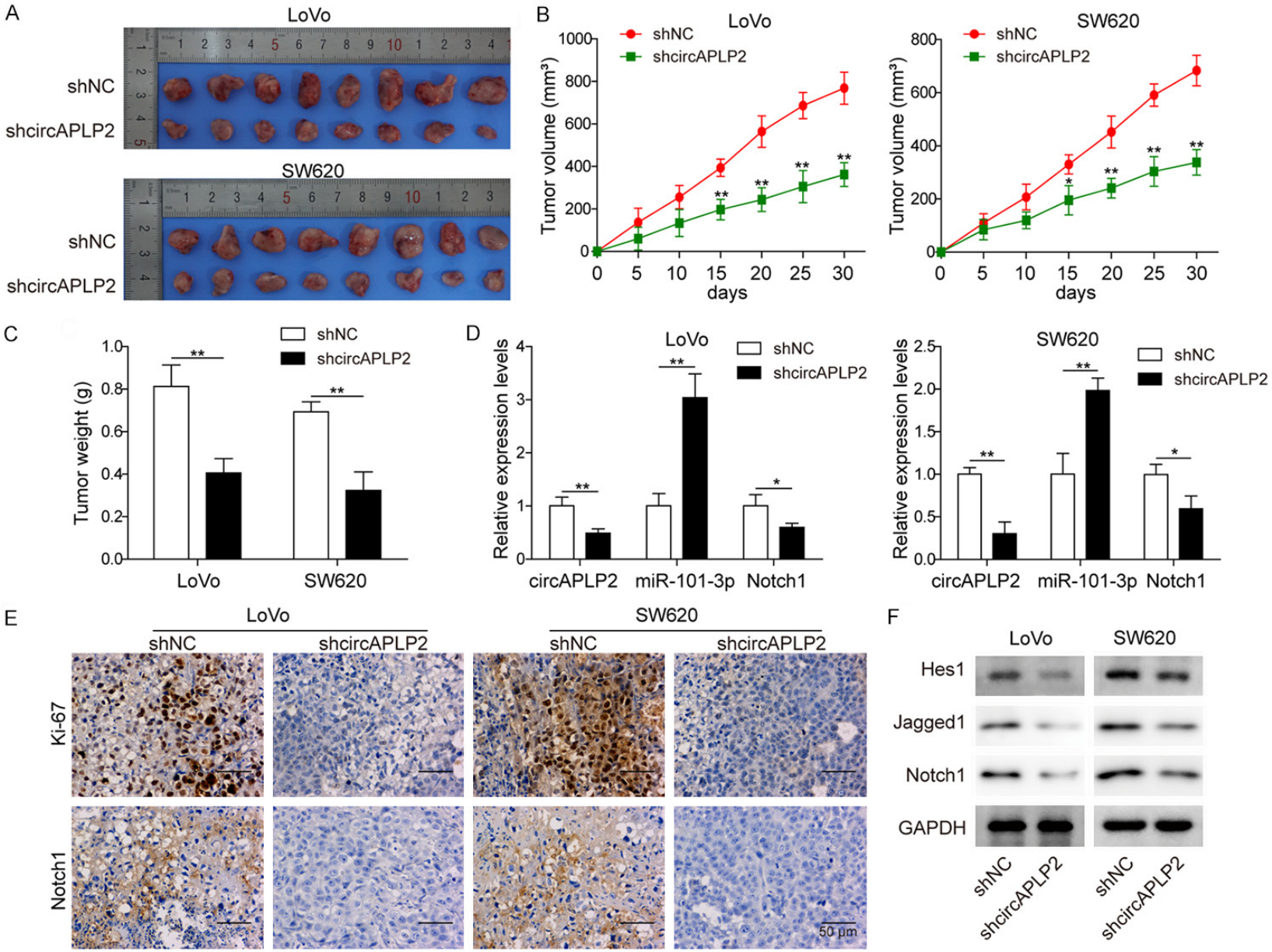
A
LoVo
shNC
shcircAPLP2
SW620
shNC
shcircAPLP2
B
LoVo
shNC
shcircAPLP2
Tumor volume (mm³)
days
SW620
shNC
shcircAPLP2
Tumor volume (mm³)
days
C
shNC
shcircAPLP2
Tumor weight (g)
LoVo
SW620
D
LoVo
shNC
shcircAPLP2
Relative expression levels
circAPLP2
miR-101-3p
Notch1
SW620
shNC
shcircAPLP2
Relative expression levels
circAPLP2
miR-101-3p
Notch1
E
LoVo
shNC
shcircAPLP2
SW620
shNC
shcircAPLP2
Ki-67
Notch1
50 μm
F
LoVo
SW620
Hes1
Jagged1
Notch1
GAPDH
shNC
shcircAPLP2
shNC
shcircAPLP2

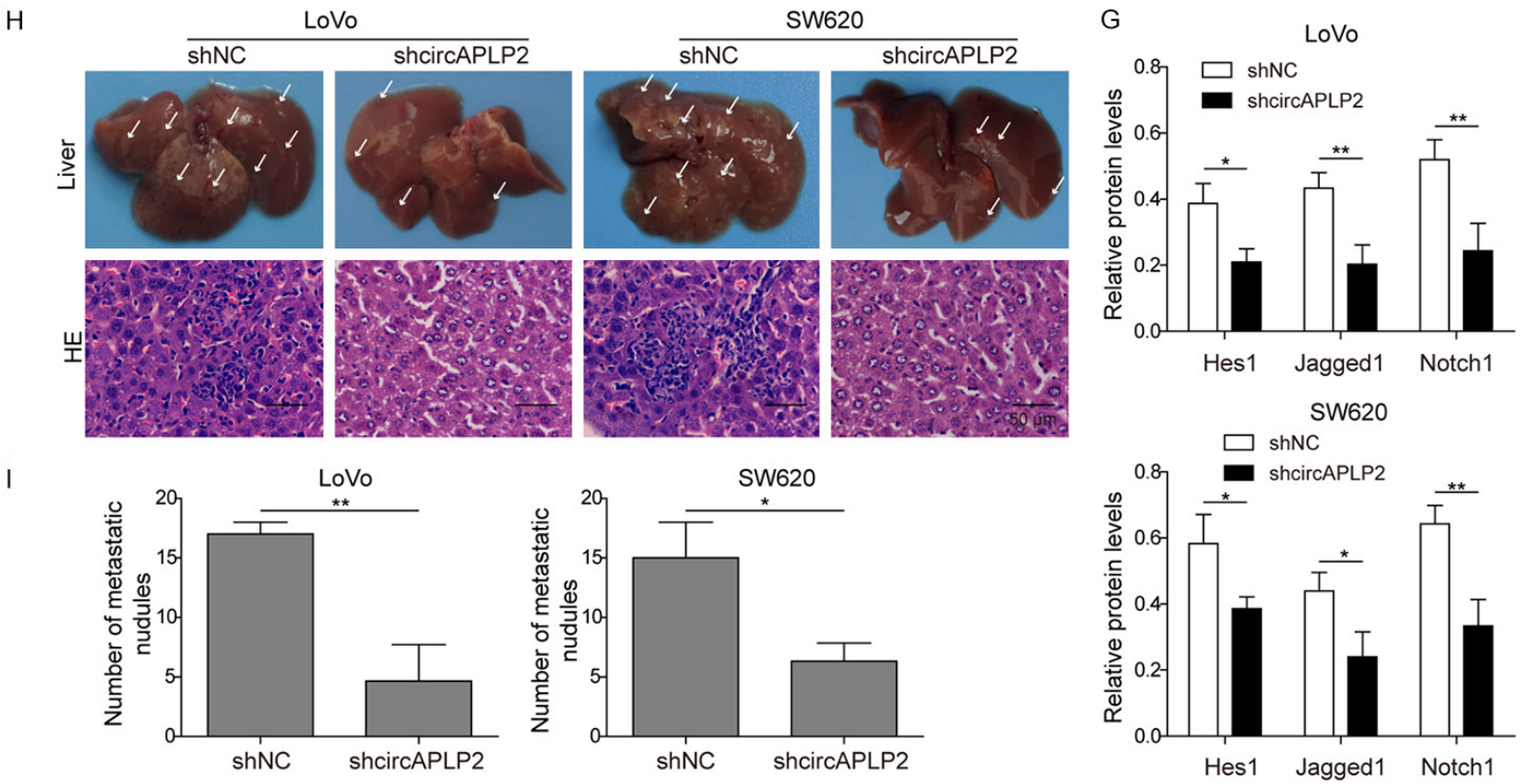

Figure 6. circAPLP2 knockdown suppressed tumour growth and liver metastasis in nude mice. (A) *In vivo* xenograft mouse model of LoVo and SW620 cells expressing control or circAPLP2 shRNAs. Representative pictures of isolated xenografts are shown. (B) *In vivo* growth of LoVo and SW620 cells expressing control or circAPLP2 shRNAs. Tumour sizes were measured every five days with an electronic calliper. (C) Weights of tumours harvested from mice at the end of experiments. (D) The expression levels of circAPLP2, miR-101 and Notch1 in xenograft tumour tissues were measured by qRT-PCR. GAPDH or U6 was used for normalization. (E) IHC staining analysis of Ki-67 and Notch1 in tumour tissues of xenograft mouse models of LoVo and SW620 cells expressing control or circAPLP2 shRNAs. (F) The protein levels of Hes1, Jagged1 and Notch1 in xenograft tumour tissues were assessed by Western blotting. (G) Greyscale values of Western blot bands in (F), and GAPDH was used for normalization. (H) Liver metastases in nude mice after tail vein injection of CRC cells and H&E staining of liver tissues. (I) The number of metastatic nodules in the livers of nude mice after tail vein injection of CRC cells. All the results are shown as the mean ± SD (n = 3). *$P < 0.05$ and **$P < 0.01$.

be downregulated in both CRC tissues and cell lines and upregulated after circAPLP2 knockdown. The direct interaction between miR-101-3p and circAPLP2 was further validated through bioinformatics analysis and luciferase assays. Furthermore, miR-101 inhibition reversed the inhibition of proliferation, migration and invasion induced by circAPLP2 knockdown. Taken together, these data indicate that circAPLP2 promotes progression and metastasis by sponging miR-101-3p.

It has been reported that abnormal Notch signalling can impact the tumorigenicity and proliferation of CRC [23]. Jagged1 (JAG1) is one of the five canonical ligands for Notch receptors, while Hes1 is one of the targets of Notch1 [32]. Notch1 was reported to promote stemness and EMT in CRC [9]. Jagged1 knockdown inhibits cell growth and invasion in CRC [8]. Another transcriptional factor in the Notch signalling pathway, HES1, promotes metastasis and predicts poor survival in patients with CRC [26]. The transcription of Notch target genes such as p21 (CDKN1A), hairy enhancer of split 1 (HES1), c-myc (MYC), HES-related proteins (HEY) and cyclin D1 (CCDN1) can be induced by the Notch intracellular domain (NICD) [33]. In addition, Notch1 signalling is dependent on the activity of MMPs [34]. Here, we revealed that the Notch signalling pathway is activated in CRC. circAPLP2 promoted Notch1 expression by directly binding to miR-101-3p. Additionally, knockdown of circAPLP2 and overexpression of miR-101-3p inhibited proliferation and metastasis-related signals, including c-Myc, cyclin D1, MMP-2 and MMP-9, by repressing the Notch signalling pathway, thereby suppressing CRC growth and liver metastasis.

In conclusion, our study provides the first clue regarding the regulatory role of circAPLP2 in CRC through the miR-101-3p/Notch1 axis. Knockdown of circAPLP2 inhibits the proliferation and metastasis of CRC by repressing the Notch signalling pathway by targeting miR-101-3p. This finding provides new insights into the mechanisms underlying CRC malignancy and suggests a new therapeutic target.

Disclosure of conflict of interest

None.

Address correspondence to: Dr. Ming Chen, Department of Gastroenterology, The First People's Hospital of Huaihua City, No. 144 Jinxi South Road, Hecheng District, Huaihua 418000, Hunan Province, P. R. China. Tel: +86-13789277927; E-mail: chenmingdd88@163.com

References

[1] Arnold M, Sierra MS, Laversanne M, Soerjomataram I, Jemal A and Bray F. Global patterns and trends in colorectal cancer incidence and mortality. Gut 2017; 66: 683-691.

[2] Simon K. Colorectal cancer development and advances in screening. Clin Interv Aging 2016; 11: 967-976.

[3] Cheng YC and Ueno NT. Improvement of survival and prospect of cure in patients with metastatic breast cancer. Breast Cancer 2012; 19: 191-199.

[4] Vinson KE, George DC, Fender AW, Bertrand FE and Sigounas G. The Notch pathway in colorectal cancer. Int J Cancer 2016; 138: 1835-1842.

[5] Andrawes MB, Xu X, Liu H, Ficarro SB, Marto JA, Aster JC and Blacklow SC. Intrinsic selectivity of notch 1 for delta-like 4 over delta-like 1. J Biol Chem 2013; 288: 25477-25489.

[6] Bolos V, Grego-Bessa J and de la Pompa JL. Notch signaling in development and cancer. Endocr Rev 2007; 28: 339-363.

[7] Wang Z, Li Y, Kong D and Sarkar FH. The role of Notch signaling pathway in epithelial-mesenchymal transition (EMT) during development and tumor aggressiveness. Curr Drug Targets 2010; 11: 745-751.

[8] Fender AW, Nutter JM, Fitzgerald TL, Bertrand FE and Sigounas G. Notch-1 promotes stemness and epithelial to mesenchymal transition in colorectal cancer. J Cell Biochem 2015; 116: 2517-2527.

[9] Weng MT, Tsao PN, Lin HL, Tung CC, Change MC, Chang YT, Wong JM and Wei SC. Hes1 increases the invasion ability of colorectal cancer cells via the STAT3-MMP14 pathway. PLoS One 2015; 10: e0144322.

[10] Qu S, Yang X, Li X, Wang J, Gao Y, Shang R, Sun W, Dou K and Li H. Circular RNA: a new star of noncoding RNAs. Cancer Lett 2015; 365: 141-148.

[11] Chen LL and Yang L. Regulation of circRNA biogenesis. RNA Biol 2015; 12: 381-388.

[12] Zhang Z, Xie Q, He D, Ling Y, Li Y, Li J and Zhang H. Circular RNA: new star, new hope in cancer. BMC Cancer 2018; 18: 834.

[13] Zhuang C, Huang X, Yu J and Gui Y. Circular RNA hsa_circ_0075828 promotes bladder cancer cell proliferation through activation of CREB1. BMB Rep 2020; 53: 82-87.

[14] Su W, Wang Y, Wang F, Sun S, Li M, Shen Y and Yang H. Hsa_circ_0005379 regulates malignant behavior of oral squamous cell carcino-

ma through the EGFR pathway. BMC Cancer 2019; 19: 400.
[15] Li XN, Wang ZJ, Ye CX, Zhao BC, Li ZL and Yang Y. RNA sequencing reveals the expression profiles of circRNA and indicates that circDDX17 acts as a tumor suppressor in colorectal cancer. J Exp Clin Cancer Res 2018; 37: 325.
[16] Li X, Wang J, Zhang C, Lin C, Zhang J, Zhang W, Lu Y and Zheng L. Circular RNA circITGA7 inhibits colorectal cancer growth and metastasis by modulating the Ras pathway and upregulating transcription of its host gene ITGA7. J Pathol 2018; 246: 166-179.
[17] Abba M, Patil N and Allgayer H. MicroRNAs in the regulation of MMPs and metastasis. Cancers (Basel) 2014; 6: 625-645.
[18] Wang Z, Li Y, Kong D, Ahmad A, Banerjee S and Sarkar FH. Cross-talk between miRNA and Notch signaling pathways in tumor development and progression. Cancer Lett 2010; 292: 141-148.
[19] Slattery ML, Herrick JS, Pellatt DF, Mullany LE, Stevens JR, Wolff E, Hoffman MD, Wolff RK and Samowitz W. Site-specific associations between miRNA expression and survival in colorectal cancer cases. Oncotarget 2016; 7: 60193-60205.
[20] Strillacci A, Valerii MC, Sansone P, Caggiano C, Sgromo A, Vittori L, Fiorentino M, Poggioli G, Rizzello F, Campieri M and Spisni E. Loss of miR-101 expression promotes Wnt/beta-catenin signalling pathway activation and malignancy in colon cancer cells. J Pathol 2013; 229: 379-389.
[21] He D, Yue Z, Li G, Chen L, Feng H and Sun J. Low serum levels of miR-101 are associated with poor prognosis of colorectal cancer patients after curative resection. Med Sci Monit 2018; 24: 7475-7481.
[22] Zeng K, Chen X, Xu M, Liu X, Hu X, Xu T, Sun H, Pan Y, He B and Wang S. CircHIPK3 promotes colorectal cancer growth and metastasis by sponging miR-7. Cell Death Dis 2018; 9: 417.
[23] Li X, Zhao X, Yang B, Li Y, Liu T, Pang L, Fan Z, Ma W, Liu Z and Li Z. Long non-coding RNA HOXD-AS1 promotes tumor progression and predicts poor prognosis in colorectal cancer. Int J Oncol 2018; 53: 21-32.
[24] Song J, Shu H, Zhang L and Xiong J. Long noncoding RNA GAS5 inhibits angiogenesis and metastasis of colorectal cancer through the Wnt/beta-catenin signaling pathway. J Cell Biochem 2019; [Epub ahead of print].
[25] Vatandoust S, Price TJ and Karapetis CS. Colorectal cancer: metastases to a single organ. World J Gastroenterol 2015; 21: 11767-11776.
[26] Bian L, Zhi X, Ma L, Zhang J, Chen P, Sun S, Li J, Sun Y and Qin J. Hsa_circRNA_103809 regulated the cell proliferation and migration in colorectal cancer via miR-532-3p/FOXO4 axis. Biochem Biophys Res Commun 2018; 505: 346-352.
[27] Guo JN, Li J, Zhu CL, Feng WT, Shao JX, Wan L, Huang MD and He JD. Comprehensive profile of differentially expressed circular RNAs reveals that hsa_circ_0000069 is upregulated and promotes cell proliferation, migration, and invasion in colorectal cancer. Onco Targets Ther 2016; 9: 7451-7458.
[28] Imamura T, Komatsu S, Ichikawa D, Miyamae M, Okajima W, Ohashi T, Kiuchi J, Nishibeppu K, Kosuga T, Konishi H, Shiozaki A, Okamoto K, Fujiwara H and Otsuji E. Low plasma levels of miR-101 are associated with tumor progression in gastric cancer. Oncotarget 2017; 8: 106538-106550.
[29] Li L, Shao MY, Zou SC, Xiao ZF and Chen ZC. MiR-101-3p inhibits EMT to attenuate proliferation and metastasis in glioblastoma by targeting TRIM44. J Neurooncol 2019; 141: 19-30.
[30] Liang H, Yu T, Han Y, Jiang H, Wang C, You T, Zhao X, Shan H, Yang R, Yang L and Gu Y. LncRNA PTAR promotes EMT and invasion-metastasis in serous ovarian cancer by competitively binding miR-101-3p to regulate ZEB1 expression. Mol Cancer 2018; 17: 119.
[31] Liu D, Li Y, Luo G, Xiao X, Tao D, Wu X, Wang M, Huang C, Wang L, Zeng F and Jiang G. LncRNA SPRY4-IT1 sponges miR-101-3p to promote proliferation and metastasis of bladder cancer cells through up-regulating EZH2. Cancer Lett 2017; 388: 281-291.
[32] Li D, Masiero M, Banham AH and Harris AL. The notch ligand JAGGED1 as a target for anti-tumor therapy. Front Oncol 2014; 4: 254.
[33] Cenciarelli C, Marei HE, Zonfrillo M, Casalbore P, Felsani A, Giannetti S, Trevisi G, Althani A and Mangiola A. The interference of Notch1 target Hes1 affects cell growth, differentiation and invasiveness of glioblastoma stem cells through modulation of multiple oncogenic targets. Oncotarget 2017; 8: 17873-17886.
[34] Fazio C, Piazzi G, Vitaglione P, Fogliano V, Munarini A, Prossomariti A, Milazzo M, D'Angelo L, Napolitano M, Chieco P, Belluzzi A, Bazzoli F and Ricciardiello L. Inflammation increases NOTCH1 activity via MMP9 and is counteracted by Eicosapentaenoic Acid-free fatty acid in colon cancer cells. Sci Rep 2016; 6: 20670.